

Combined Solar Chimney Power Plant and Solar Still

Assist. Prof. Dr. Salman H. Hammadi

*University of Basrah-engineering college
Mechanical Engineering department
Salman.hammadi@unobasrah.edu.iq*

Abstract- This study presents solar chimney power plant integrated with sea water desalination system. A simple mathematical model is based on the conservation of mass and energy. The results show that the integrated system of solar chimney power plant and solar still can achieve simultaneously. The analysis is performed for both summer and winter at latitude 30°N. It's noted that, the water layer thickness is of a significant effect on the fresh water productivity while the dimensions of solar chimney and the solar collector are of a minor effect. The productivity of fresh water and output power for summer are the highest. The present work is compared with experimental data of the other work and showed a good agreement.

Index Terms-solar chimney, solar still, desalination, water purification.

1. INTRODUCTION

In warm countries, energy and fresh water demand increasingly. In classical power plants and desalination unit, pollution increases and high fuel consumption is required. So the ideal solution is to use renewable energy. Solar energy is one of the most frequently used to drive renewable power plant and desalination units in an environmentally friendly manner. Many researchers studied the solar power plant and solar still separately but there is a few others integrated both solar power generation and solar still units.

Y.J. Dai et.al [1] studied solar chimney power plant in northwestern China. They presented a simple theoretical model. Solar power plant chimney, in which the height and diameter of the chimney are 200 m and 10 m, respectively, and the diameter of the solar collector cover is 500 m, is able to produce 110~190 kW electric power on a monthly average all year. Some parameters, such as chimney height, diameter of the solar collector, ambient temperature, solar irradiance and the efficiency which influence the performance of power generation, are also analyzed. Mohammad O.Hamdan [2] presented A simplified thermodynamics analytical model for steady air flow inside a solar chimney in Arabian gulf region. The results show that a solar chimney power plant with a chimney height of 500 m and a collector

roof diameter of 1000 m would produce at least 8 MW of power. He concluded that, the amount of power produced during the summer would be higher where the demand in the Gulf area is the highest.

Lu zuo et. al 2011 [3] developed a new mathematical model to solar chimney power system with integration of sea water desalination in Northwest China. Through theoretical analysis, it has been demonstrated the integrated system can significantly improve the solar energy utilization efficiency as well as the land resources utilization efficiency, at the same time, the economic, social and ecological benefits can also be significant.

Lu zuo et. al 2011 [4] presented a small-scale experimental device for solar chimneys integrated with sea water desalination based on the practical weather condition.

The experimental results show that the integrated system can achieve simultaneously the multi targeted production indeed, such as power and freshwater. The main period of the distilled water output is during the absence of solar irradiance, but the minimum output is during the period of the strong radiance. The airflow temperature rises along the radial of the system and the temperature rise mainly occurs in the first 1/3 section of the heat collector radius. Compared to the solo solar chimney power generation system, the integrated system would significantly improve the utilization efficiency of the solar energy.

II. THEORETICAL ANALYSIS

In order to simplify the theoretical analysis, the following assumptions can be considered:

1. The temperature distribution inside the solar collector is linear.
2. No heat transfer from the basin of the solar still to ground.
3. Thermal properties of air is constant except the density is temperature dependent.

4. No temperature gradient along the solar chimney.

Fig. 1 shows the theoretical model which combined solar chimney power plant and solar still. The energy balance equations of different components of the system can be considered as follows:

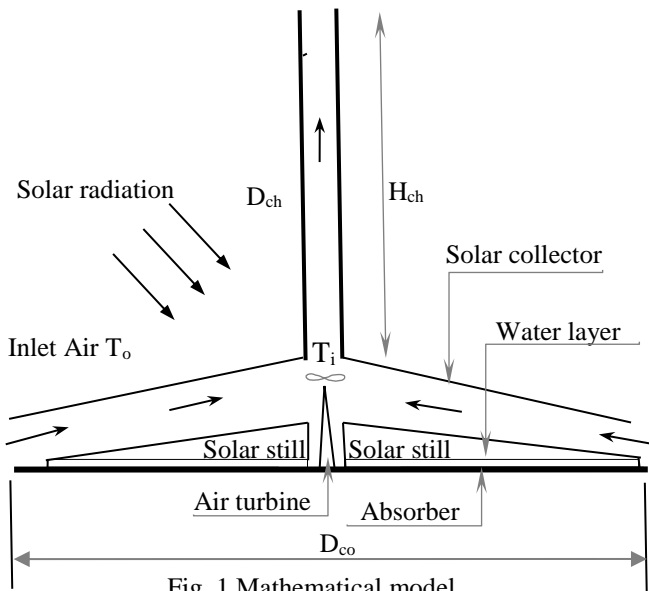


Fig. 1 Mathematical model

Water layer

$$\alpha_w I A_c + h_w A_c (T_b - T_w) - h_{wg} A_c (T_w - T_g) = m_w C_w \frac{dT_w}{dt} \tag{1}$$

Solar still glass cover

$$h_{wg} (T_w - T_g) = h_g (T_g - T_{iav}) \tag{2}$$

Absorber plate

$$\alpha_b I = h_w (T_b - T_w) \tag{3}$$

The energy balance for the air stream enters the solar collector can be given as:

$$h_{wg} A_c (T_w - T_g) - h_o A_c (T_{iav} - T_o) = m_a C_a (T_i - T_o) \tag{4}$$

Where;

$$T_{iav} = \frac{T_i + T_o}{2} \tag{5}$$

The pressure difference produced between chimney base and the surroundings is given as:

$$\Delta p = g \int_0^{H_{ch}} (\rho_o - \rho_i) dz \tag{6}$$

For constant density difference along the chimney, the last equation can be written as:

$$\Delta p = g (\rho_o - \rho_i) H_{ch} \tag{7}$$

By using the Boussinesq approximation, the air density difference can be calculated by [5]:

$$\rho_o - \rho_i \approx \rho_o \beta \Delta T \tag{8}$$

Applying Bernoulli equation along the chimney, the air mass flowrate is given as follows:

$$\dot{m}_a = \rho_i A_{ch} \sqrt{\frac{2 g H_{ch} (T_i - T_o)}{T_o}} \tag{9}$$

The direct solar radiation flux that incident on the solar collector can be gives as a sine wave profile as follows:

$$I = A \sin \frac{\pi t}{D} \tag{10}$$

Where;

(A) is maximum direct solar radiation during the day.

(t) is the time from the sunrise.

(D) is the day length (time interval from the sunrise to sunset).

The heat transfer coefficient between the water layer and the glass cover is given as [6]:

$$h_{wg} = h_{cw} + h_{rw} + h_{ew} \tag{11}$$

Where;

$$h_{cw} = 0.884 \left[T_w - T_g + (P_w - P_g) \frac{(T_w + 273)}{(268.9 \times 10^3 - P_w)} \right]^{1/3} \tag{11 a}$$

$$h_{rw} = \epsilon \sigma \frac{[(T_w+273)^4 - (T_g+273)^4]}{(T_w - T_g)} \quad (11 \text{ b})$$

$$h_{ew} = 16.273 \times 10^{-3} h_{cw} \frac{(P_w - P_g)}{(T_w - T_g)} \quad (11 \text{ c})$$

And ;

$$P_w = \exp \left[25.317 - \frac{5144}{(T_w + 273)} \right] \quad (12 \text{ a})$$

$$P_g = \exp \left[25.317 - \frac{5144}{(T_g + 273)} \right] \quad (12 \text{ b})$$

The heat transfer coefficient inside the solar collector can be give as [7]:

$$h_o = 5.7 + 3.8 \bar{u} \quad (13)$$

Where; \bar{u} is the average air velocity inside the solar collector which can be evaluated from the following formula:

$$\bar{u} = \frac{\dot{m}_a}{2\pi\bar{\rho}(r_{co} - r_{ch})} \int_{r_{ch}}^{r_{co}} \frac{dr}{r} \quad (14)$$

$$\bar{u} = \frac{\dot{m}_a}{2\pi\bar{\rho}(r_{co} - r_{ch})} \ln \frac{r_{co}}{r_{ch}} \quad (15)$$

Equation (1) can be written as:

$$\frac{dT_w}{dt} = \frac{\alpha_w I A_c + h_w A_c (T_b - T_w) - h_{wg} A_c (T_w - T_g)}{m_w C_w} \quad (16)$$

The last Equation can be solved numerically using equations (2 to 15) to evaluate temperature of the water layer at any time.

And the hourly productivity of the solar still is given as:

$$\dot{m}_{ew} = \frac{3600 h_{ew} (T_w - T_g)}{h_{fg}} \quad (17)$$

The daily productivity is given by:

$$M_{ew} = \sum_{i=1}^{24} \dot{m}_{ew} \quad (18)$$

The available power due to the upward hot air stream can be given as:

$$P = \frac{1}{2} \frac{\dot{m}_a^3}{(\rho A_{ch})^2} \quad (19)$$

III. RESULTS AND DISCUSSION

The calculations are performed at latitude 30°N for January and July .The values of the parameter (A) that is appeared in equation (10) are considered to be 600 W/m² for January and 900 W/m² for July. All calculations are performed using matlab software.

Fig.2 shows the water, air, and glass cover temperature as a function of time in January. The temperatures increase with time to reach maximum value before falling down gradually. It is clear they affected by the solar radiation intensity profile. Fig. 3 shows a similar behavior but higher values of water, air, and glass temperatures than that shown in January due to the higher solar radiation intensity in July.

Figures.4 and 5 show the output power in January and July. It's clear that the output power increase with increasing of the chimney height due to the increase of the draft force as the chimney height increases. Also the output power in summer is the highest due to the highest solar radiation intensity in summer.

In figures 6 and 7, the output power increases with increasing chimney diameter due to the increase of air mass flowrate. The curves order is changed after about 4 hrs. from mid-day. This is because the decrease of solar intensity afternoon and the effect of the heat capacity of water layer.

Figure 8 and 9 show that the power generated is significantly increase with increasing the collector diameter due to increase of the solar radiation absorbed by the collector. It is also show the output power in summer is about two time that of winter.

Figures 10 and 11 show that, the output power is inversely proportional to the water layer depth during the day due to the fast and easiest heating of a small quantity of water in comparison with the large one. At night the smallest mass of water which is considered as heat storage cooled faster which means low air temperature inside the collector and in turn, low power generated.

Figures 12 and 13 show the productivity of the solar still with time for different values of chimney height.

Its shows a slightly increase of the productivity with increase of chimney height during the day this is because that, the air velocity inside the collector increases with increasing chimney height and in turn

increases heat losses from the still glass cover causing an increase of the condensation rate. On the other hand this may be increasing the heat losses from the water layer which means a decrease in the condensation potential. At night show an inflection in the behavior due to the effect of heat capacity of the water layer. It's also show that the productivity in summer is much higher than that of winter due to high solar intensity and evaporation potential in summer.

Figures 14 and 15 show a slightly increase in productivity with increase of chimney diameter due to increase of the mass flowrate which in turn increase of heat transfer coefficient in the collector and decrease the still glass cover temperature causing increase of condensation potential. At night, where absence of the solar radiation, heat capacity of the water layer causes an inflection in the curves behavior.

Figures 16 and 17 show a decrease in the productivity with increasing the collector diameter this may be due to the increase of the air mass flowrate and in turn increase of heat losses from the water layer in the still causing a decrease in the evaporation potential.

Figures 18 and 19 show a significant increase in the productivity with decreasing water layer depth due to low heat resistance of the small water layer thickness and easy to heating and in turn increase of evaporation potential.

A comparison between fresh water productivity of the present work and experimental data of the work by Tiwari et.al.[6] is shown in Fig.20. The comparison was made for variable solar radiation along the day where the maximum value at mid-day is 696 W/m^2 . It shows a good agreement between the two works.

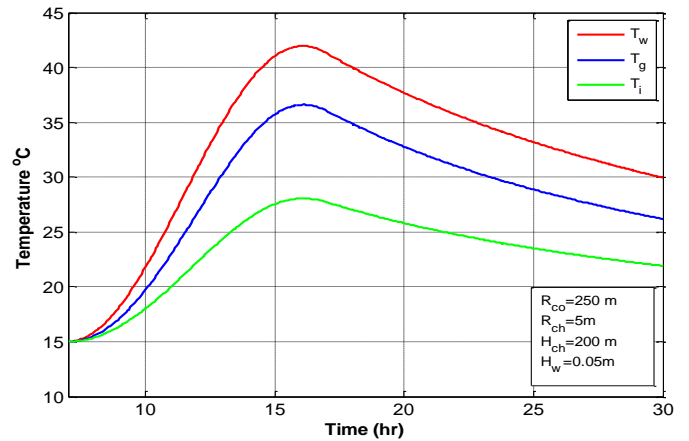


Fig.2 Temperature profile of water layer, still glass cover and inside collector air (January).

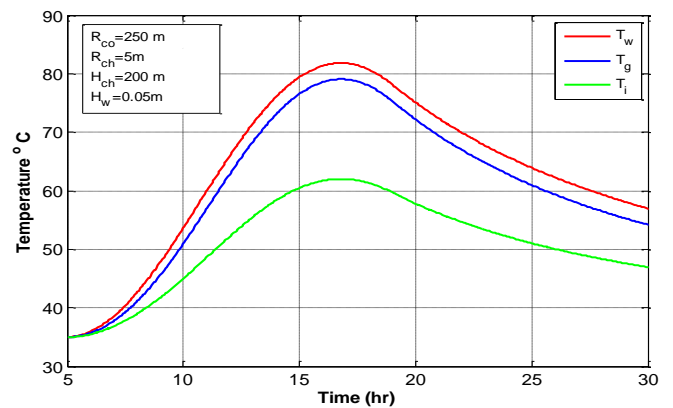


Fig.3 Temperature profile of water layer, still glass cover, and inside collector air (July).

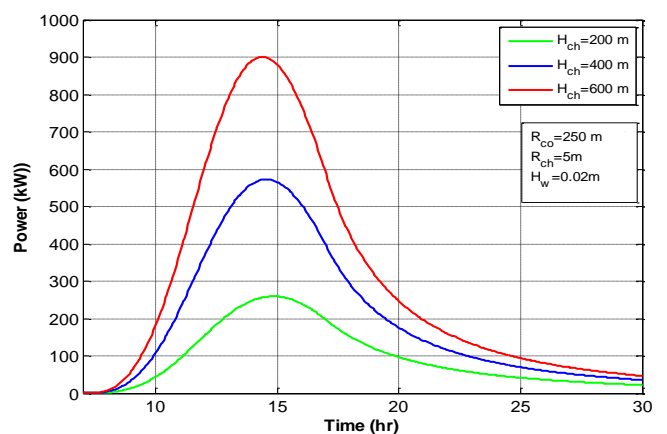


Fig.4 Effect of chimney height on output power (January).

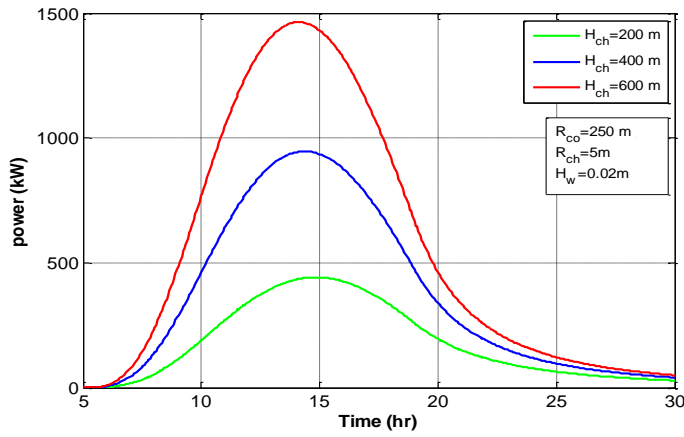


Fig.5 Effect of chimney height on output power (July).

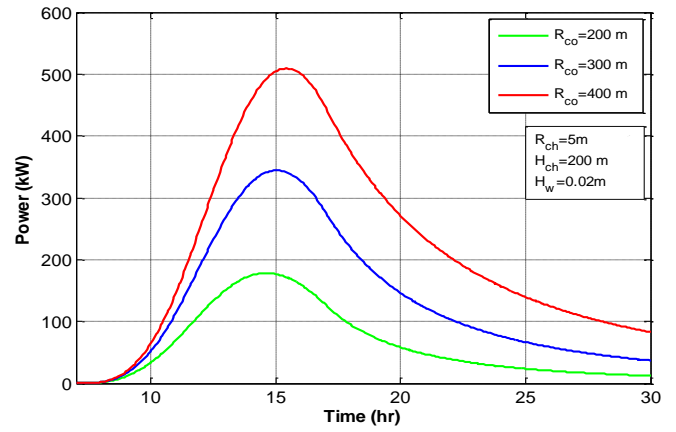


Fig.8 Effect of collector radius on output power (January).

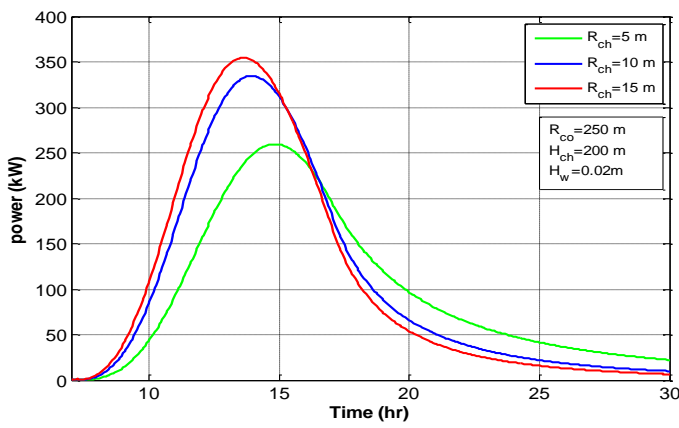


Fig.6 Effect of chimney radius on output power (January).

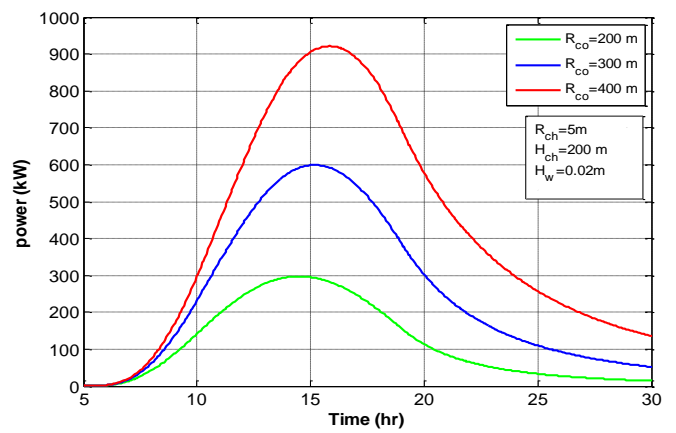


Fig.9 Effect of collector radius on output power (January).

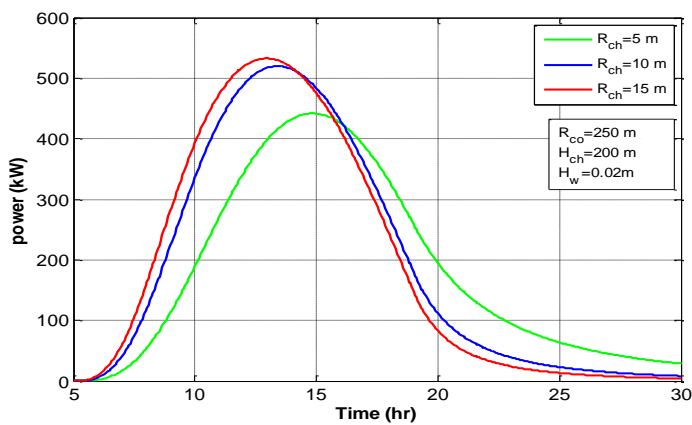


Fig.7 Effect of chimney radius on output power (July).

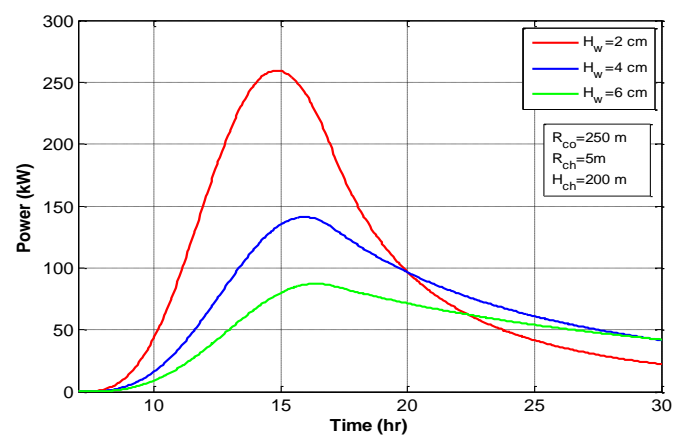


Fig.10 Effect of water layer thickness on output power (January).

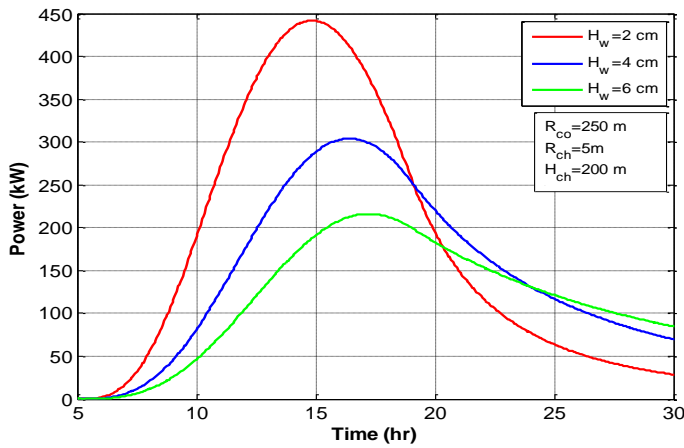


Fig.11 Effect of water layer thickness on output power (July).

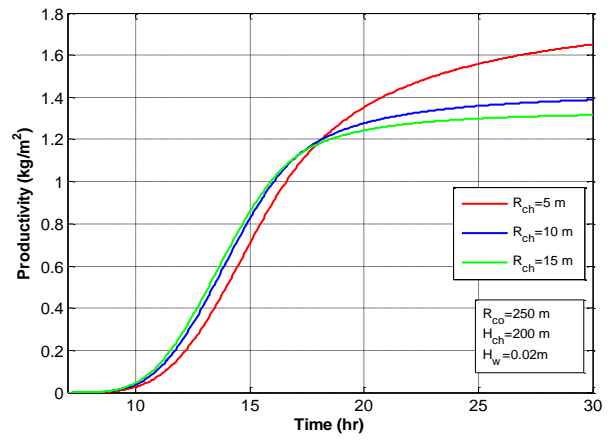


Fig.14 Effect of chimney radius on productivity (January).

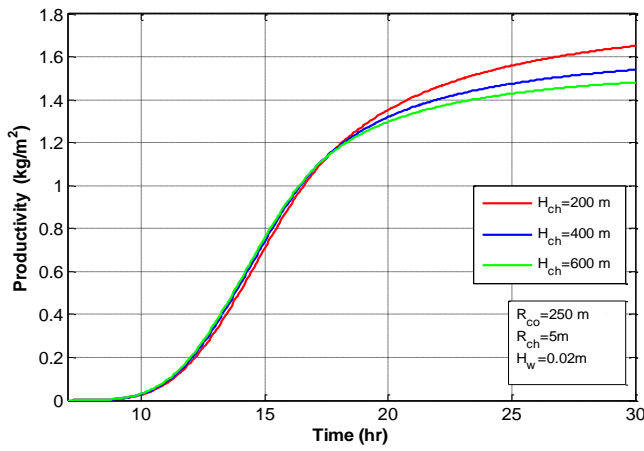


Fig.12 Effect of chimney height on productivity (January).

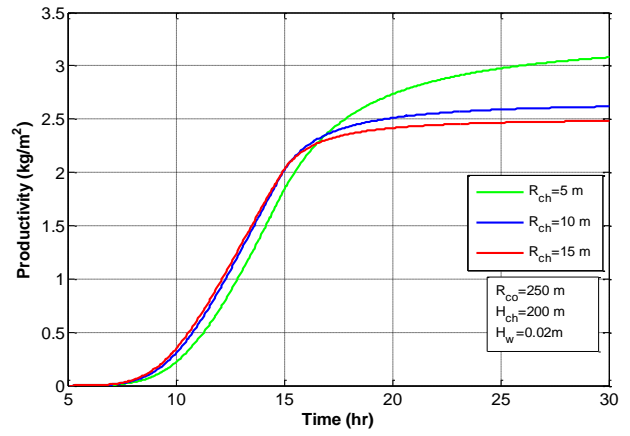


Fig.15 Effect of chimney radius on productivity (July).

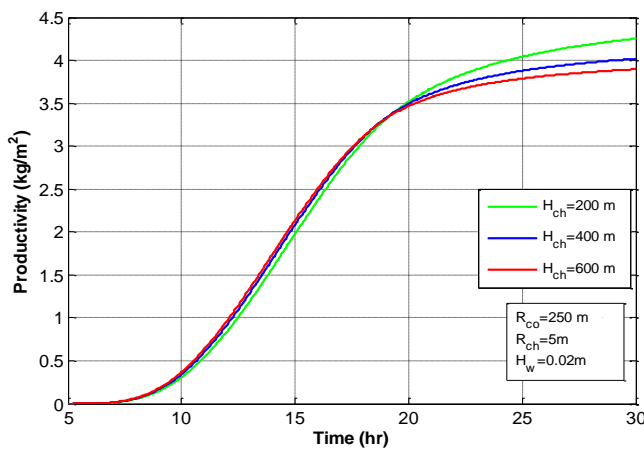


Fig.13 Effect of chimney height on productivity (July).

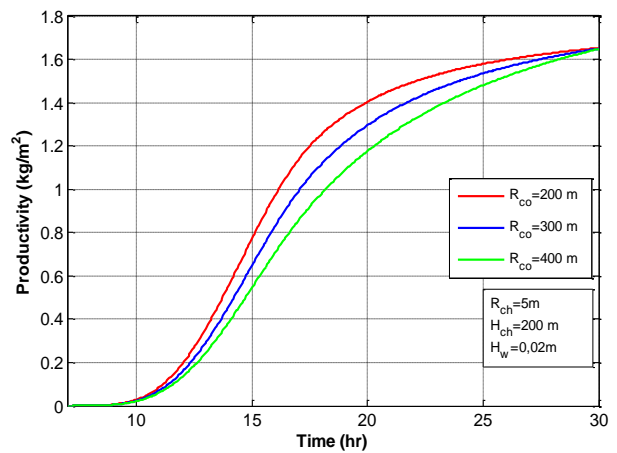


Fig.16 Effect of collector radius on productivity (January).

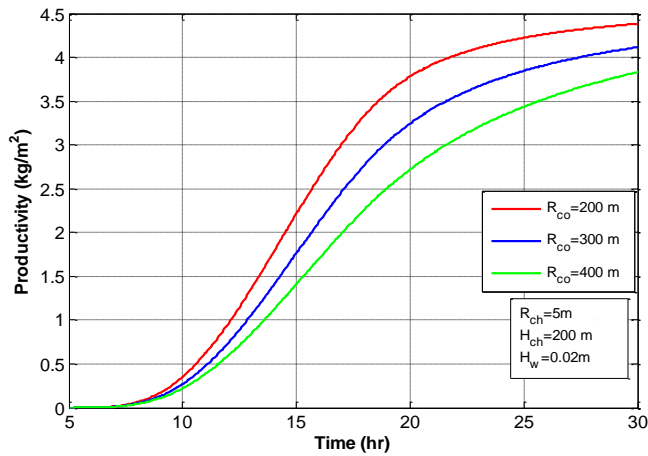


Fig.17 Effect of collector radius on productivity (July).

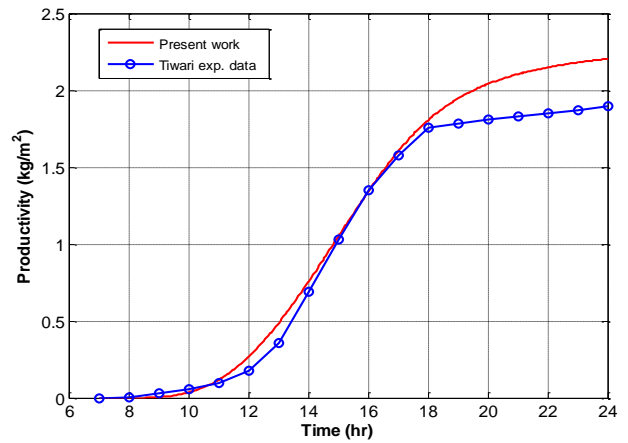


Fig.20 comparison productivity of the present work and experimental data of Tiwari [6].

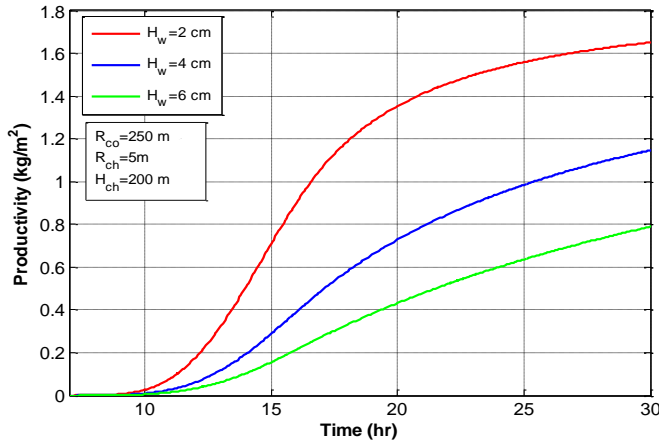


Fig.18 Effect of water layer thickness on productivity (January).

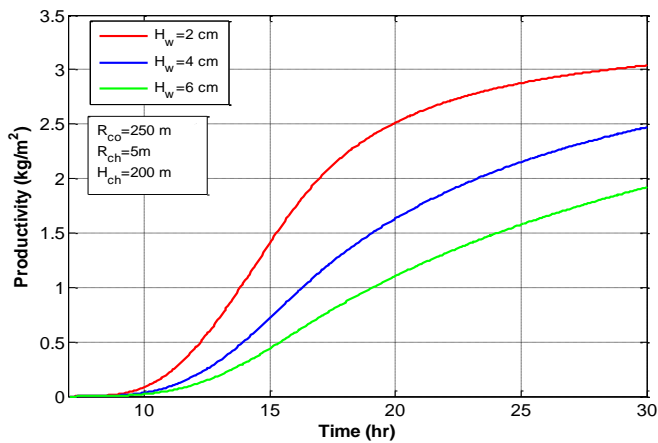


Fig.19 Effect of water layer thickness on productivity (July).

IV. CONCLUSIONS

The present work leads to the following conclusions:

1. The combined system to product power and freshwater driven by solar energy can achieve.
2. The productivity of fresh water is affected significantly by water layer thickness.
3. The chimney and collector dimensions are of a significant effect on the output Power especially the chimney height.
4. A slight effect of the system dimensions on the productivity of fresh water per unit area.
5. The output Power and productivity of fresh water in the summer are higher than that of winter.

5. REFERENCES

- [1] Y.J. Dai., H. B Huang., and R. Z Wang., "Case study of solar chimney power plants in Northwestern regions of China" J. Renewable Energy, vol.28, pp.1295-1304. 2003.
- [2] Mohammad O. Hamdan, "Analysis of a solar chimney power plant in the Arabian Gulf region" Renewable Energy, vol.xxx, pp1-6. 2010.
- [3] Lu Zuo, Yuan Zheng, Li Zhenjie and Yujun Sha, "Solar chimneys integrated with sea

water desalination” J. Desalination, vol.276, pp. 207- 2013, 2011.

- [4] Lu Zuo, Yuan Zheng, Zhenjie Li and Yujun Sha, “Experimental research on solar chimneys integrated with seawater desalination under practical weather condition” J. Desalination, vol.298, pp. 22-33, 2012.
- [5] Penghua Guo, Li Jingyin, Yunfeng Wang, Yuan Wang,” Evaluation of the optimal turbine pressure drop ratio for a solar chimney power plant”, J. Energy Conversion and Management, vol.108, pp. 14-22. 2016.
- [6] Rajesh tripathi and G. N. Tiwari, “Performance evaluation of a solar still by using the concept of solar fractionation” J. Desalination, vol.169, pp. 69-80, 2004.
- [7] S. Zeinab Abdel-Rehim, Ashraf Lasheen, “Experimental and theoretical study of a solar desalination system located in Cairo Egypt” J. Desalination, vol.217, pp. 52-64, 2007.

Symbols

A Parameter appears in eq. (10)
 A_c Collector area, m^2
 A_{ch} Solar chimney cross section area, m^2
 C_a Specific heat of air, $kJ/kg\ ^\circ C$
 C_w Specific heat of water, $kJ/kg\ ^\circ C$
D Day length, hr.
 D_{ch} Solar chimney diameter, m
 D_{co} Solar collector diameter, m
 h_{fg} Latent heat of vaporization, J/kg
 h_g Inside collector heat transfer coefficient, $W/m^2\ ^\circ C$
t: Time, sec.
 h_w Inside still heat transfer coefficient, $W/m^2\ ^\circ C$
 h_o Outside air heat transfer coefficient, $W/m^2\ ^\circ C$
 h_{cw} Convective heat transfer coefficient, $W/m^2\ ^\circ C$
 h_{ew} Evaporative heat transfer coefficient, $W/m^2\ ^\circ C$
 h_{rw} Radiative heat transfer coefficient, $W/m^2\ ^\circ C$
I Direct normal solar radiation, W/m^2
 \dot{m}_a Air mass flow rate, kg/s
 m_w Mass of water layer, kg
 P_w vapor pressure at water temperature, N/m^2
p Power, W
 P_g Vapor pressure at still glass

temperature, N/m^2
 r_{ch} Radius of chimney, m
 r_{co} Radius of collector, m
 T_b Absorber temperature, $^\circ C$
 T_g Still glass cover temperature, $^\circ C$
 T_i Inside collector air temperature, $^\circ C$
 T_{iav} Average inside collector air temperature, $^\circ C$
 T_o Ambient temperature, $^\circ C$
 \bar{u} Average air velocity inside collector, m/s

Greek

ρ_i Air density at chimney entrance, kg/m^3
 $\bar{\rho}$ Average air density (kg/m^3)
 α_b Absorptivity of still basin liner
 α_w Absorptivity of water layer
 ϵ Emissivity
 σ Boltzman constant